Int J Clin Exp Pathol 2017;10(1):80-87
www.ijcep.com /ISSN:1936-2625/IJCEP0040313

Original Article

Expression of vascular endothelial growth factor and hypoxia-inducible factor 1α in rat traumatic lung injury

Jianbin Cui[1], Liyuan Hu[2], Shuli Sun[1], Zhonghui Huang[1], Haitao Jiao[1]

[1]*Department of Emergency,* [2]*The Intensive Care Unit, Eighty-Ninth Hospital of PLA, Weifang, Shandong, China*

Received September 9, 2016; Accepted November 1, 2016; Epub January 1, 2017; Published January 15, 2017

Abstract: Hypoxia-inducible factor 1α (HIF-1α) is an important transcription factor in mediating oxygen homeostasis that can regulate vascular endothelial growth factor (VEGF) gene transcription. HIF-1α can induce neovascularization in ischemic injury. This research observed HIF-1α and VEGF expression in traumatic lung injury (TLI) to discuss their correlation. Healthy male SD rats at 7-week old were randomly divided into control (A) and traumatic group (B). TLI model was established by multi-function small biological tapping machine. Abbreviated injury scale (AIS), respiration, blood pressure (BP), and heart rate were monitored. Lung tissue was extracted at 6, 24, 48, 72, and 96 hours after injury to observe the pathological morphology. Myeloperoxidase (MPO) was measured by spectrophotometry. Pulmonary microvascular permeability was detected by fluorescence spectrophotometry. VEGF protein was tested by ELISA. HIF-1α protein expression was determined by Western blot. MPO activity, pulmonary microvascular permeability, VEGF, and HIF-1α protein expression were significantly higher at 6, 24, 48, 72, and 96 hours after injury compared with group A ($P < 0.05$). MPO activity reached peak at 24 h, microvascular permeability reached peak at 6 h, and VEGF and HIF-1α reached peak at 48 h after injury. They gradually decreased after that and got close to pre-injury level. VEGF and HIF-1α protein expression presented positive correlation at different time points ($r = 0.759$, $P < 0.05$). HIF-1α and VEGF protein elevated after TLI. HIF-1α may protect cell tolerance to hypoxia and promote injured vascular repair and regeneration through regulating VEGF expression.

Keywords: TLI, HIF-1α, VEGF, correlation

Introduction

Trauma shows a trend of increase year by year with social development. Trauma has become an important factor of death, while the incidence of chest trauma caused by traffic accidents was as high as 40% [1, 2]. Hemorrhagic shock and severe primary injury, including traumatic wet lung and acute pulmonary contusion, are the leading cause of early death after trauma. Important viscera secondary injury and inflammatory response are the important reason of traumatic death in late period [3, 4]. Severe chest trauma is often complicated with traumatic acute lung injury (ALI) and even acute respiratory distress syndrome (ARDS). It was showed that inflammation after trauma aggravated the lung injury. The main mechanism of ALI is lung ischemia-reperfusion, inflammatory reaction, and excessive apoptosis of alveolar epithelial cells [5, 6]. Direct damage after severe chest injury leads to acute alveolar cell death. Lung tissue ischemia hypoxia after trauma causes secondary lung injury, leading to delayed alveolar cell apoptosis. Fibroblasts fill-in causes pulmonary fibrosis after local cell apoptosis. HIF-1α is an important transcription factor to regulate oxygen homeostasis. It can regulate various target genes transcription, such as nitric oxide synthase and VEGF. Lung tissue post-traumatic ischemia hypoxia mediates alveolar epithelial cell apoptosis through HIF-1α. Inflammation aggravates after ALI, further increase HIF-1α expression. HIF-1α overexpression promotes inflammatory factor expression, thus exacerbates ALI inflammation [7, 8]. Lung tissue ischemia hypoxia and inflammatory stimulation during ALI increase vascular permeability, leading to lung edema. The role of HIF-1α in regulating pulmonary vascular permeability is still unclear. HIF-1α in ischemic injury can induce neovascularization. HIF-1α protein overexpression in rat ischemia reperfusion model is related to vascular barrier damage aggravation

and VEGF protein elevation. HIF-1α may have a dual role in blood vessel barrier protection and damage [9, 10]. Currently, HIF-1α and VEGF are mainly explored in brain and heart ischemic disease research, while their functions in TLI are still lack of investigation. This study established rat TLI model using multi-function small biological tapping machine and observed HIF-1α and VEGF expression to discuss their correlation.

Materials and methods

Experimental animal and grouping

Healthy male SD rats in 7-week old and weighted 220~240 g were provided by Shandong University, animal experiment center (license SYXK-2013-0025) and raised in SPF animal laboratory. Food and drink were in accordance with GB14925-2010 experimental animal standard. The rats were randomly divided into control (n = 30) and traumatic group (n = 75). TLI model was established by multi-function small biological tapping machine.

Rats were used for all experiments, and all procedures were approved by the Animal Ethics Committee of Eighty-ninth hospital of the Chinese people's liberation army.

Main reagents and instruments

MPO kit was purchased from Nanjing Jiancheng Bioengineering Institute. Chloral hydrate and paraformaldehyde was purchased from Tianjin Kermel chemical reagent co., Ltd. VEGF ELISA kit was purchased from Nanjing Jiancheng Bioengineering Institute. Rabbit anti rat HIF-1α monoclonal antibody was purchased from Boster. Horseradish peroxidase labeling goat anti rabbit secondary antibody was purchased from CST. DAB staining kit was purchased from ZSbio. Multi-function small biological tapping machine (BIM-III) was purchased from field surgery research institute in the third military medical university. Power Lab physiological recorder was purchased from AD Instruments Shanghai Trading Co., Ltd. Quantity One image analysis software was from BIO-RAD. Microplate reader (Multiskan MK3) was purchased from Thermo Fisher.

Animal modeling

The rat was fasted but free water at 8 h before experiment. The rat was anesthetized by 10% chloral hydrate intraperitoneal injection at 45° of left lateral position. The rat was fixed on the plate with right forelimb uplift and abduction. The third and fourth intercostal space in anterior axillary line was selected as the impact point and the skin was prepared. Multi-function small biological tapping machine was used to strike at 350 kpa pressure, with the distance at 18 cm and cylindrical metal slug quality at 22 g and diameter at 1.1 cm. The rats in control received no injury after anesthesia and obtained data at the same time with traumatic group.

General condition observation

The spirit, activity, and appetite, respiratory, heart rate (HR), and blood pressure (BP) of rat were recorded before injury. The rats died within 10 min after injury were recorded as immediate death. The lung tissue and blood gas were extracted from survival rats at 6, 24, 48, 72, and 96 h after injury.

Abbreviated injury scale (AIS)

AIS was used to evaluate lung injury after trauma referring to Organ Injury Scaling and AIS-2005 standard blunt injury assessment method. The classification increased 1 when the lesion was bilateral. AIS was between 1~6. Score 1, chest wall appeared ecchymosis and extravasated blood; lung appeared punctate hemorrhage and bleeding within one lobe. Score 6, multiple ribs fracture leading to flail chest; unilateral lung destruction; massive hemothorax; hilus pulmonis angiorrhexis.

Hematoxyline-eosin (HE) staining

The rat was killed after blood extraction from aorta abdominalis. Chest injury was observed and the lung tissue gross change was recorded. Contusion area and non-contusion area of right lung and the whole left lung tissues were fixed in paraformaldehyde and sliced at 2 mm. After embedded in paraffin, the section was stained by HE and observed under the microscope.

Lung wet/dry ratio (LW/DR)

Bilateral lung tissue was weighted and then baked at 110°C till constant weight to calculate LW/DR.

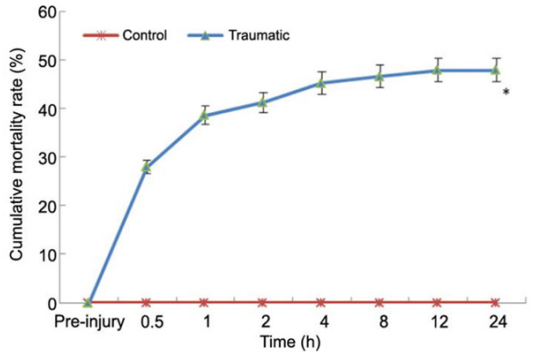

Figure 1. Cumulative mortality rate of rats after injury. *P < 0.05, vs control.

MPO activity detection

Lung tissue was extracted at 6, 24, 48, 72, and 96 h after injury and washed by precooling normal saline. Then the tissue was weighted after sipping up the surface moisture. Next, the tissue was prepared as homogenate and centrifuged at 3500 r/min for 10 min to obtain supernatant. Protein was quantified by coomassie brilliant blue. MPO activity was detected at 460 nm according to the manual.

Pulmonary microvascular permeability detection

1% sodium fluorescein at 2 ml/kg was injected through caudal vein at 15 min before each time point. The left atrium was opened and washed by normal saline upon right ventricle pressure perfusion. 50 mg left and right lung tissues were prepared as homogenate to obtain supernatant. Fluorescence spectrophotometry (slit 5 mm, excitation wavelength 437 nm, and emission wavelength 518 nm) was applied to detect the fluorescence intensity and calculate sodium fluorescein content.

ELISA

Lung tissue was homogenized to obtain supernatant. The supernatant was tested by ELISA kit according to the manual, detected at 450 nm, and calculate VEGF concentration upon standard curve.

Western blot

Total protein was extracted from the lung tissue by RIPA and quantified by BCA method. The protein was separated by SDS-PAGE at 75V for 25 min and 110V for the left. After transferred to PVDF membrane at 110V for 45 min, the membrane was blocked by blocking buffer for 1 h. Next, the membrane was incubated in primary antibody at 4°C overnight (HIF-1α 1:100, β-actin 1:200). After washed by TBST for three times, the membrane was further incubated in secondary antibody for 1 h (1:1000). At last, the membrane was treated by ECL chemiluminiscence reagent and developed. Quantity One was applied to analyze the protein bind.

Statistical analysis

SPSS 20.0 software was used for data analysis. Measurement data was first tested by normality test. The data in normal distribution was depicted as mean ± standard deviation ($\bar{x}$ ± S) and compared by one-way ANOVA or LSD test. P < 0.05 was considered as statistical significance.

Results

General condition and AIS score

The rats appeared shortness of breath, oral cyanosis, decreased activity, and depression after injury. Strong precordia ventricular beats and slow frequency could be touched in early period after injury. Some severe cases appeared bloody discharge in mouse and nose, chill, and sighing breathing. The incidence of lung injury in traumatic group was 100%. The mortality rate at 1 h after injury was 38.67% (29/75), while it was 48% (36/75) at 24 h after injury. The rats died in early period were mainly because of hemorrhagic shock, irreversible respiratory arrest, tension pneumothorax, and pulmonary hemorrhage asphyxia, etc. AIS score in rats after injury was 4.16 ± 0.22, and the mortality rate within 24 h was shown in **Figure 1**. The lesions were mainly on right upper lobe as bleeding consolidation. Whole lung and local hematoma could be observed. Laceration was found on the surface of lung tissue. Ribs indentation was showed. Right middle and lower lobes were involved in severe case (**Figure 2**).

Respiration, BP, and HR changes after injury

Rat respiration, BP, and HR were continuous monitored. Rat HR and respiration increased after injury and reached peak at 6 h. They gradually reduced and back to the pre-injury level at

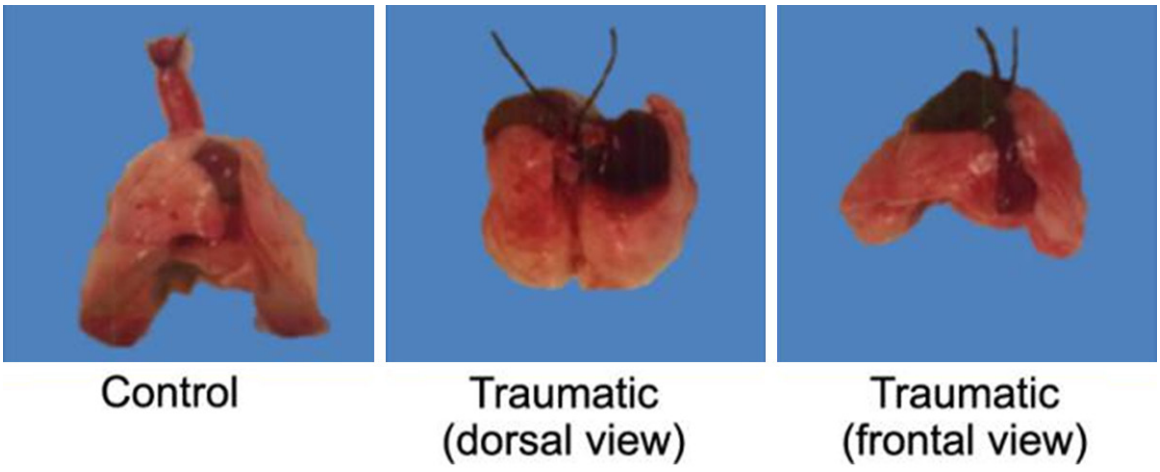

Figure 2. Gross observation of lung tissue.

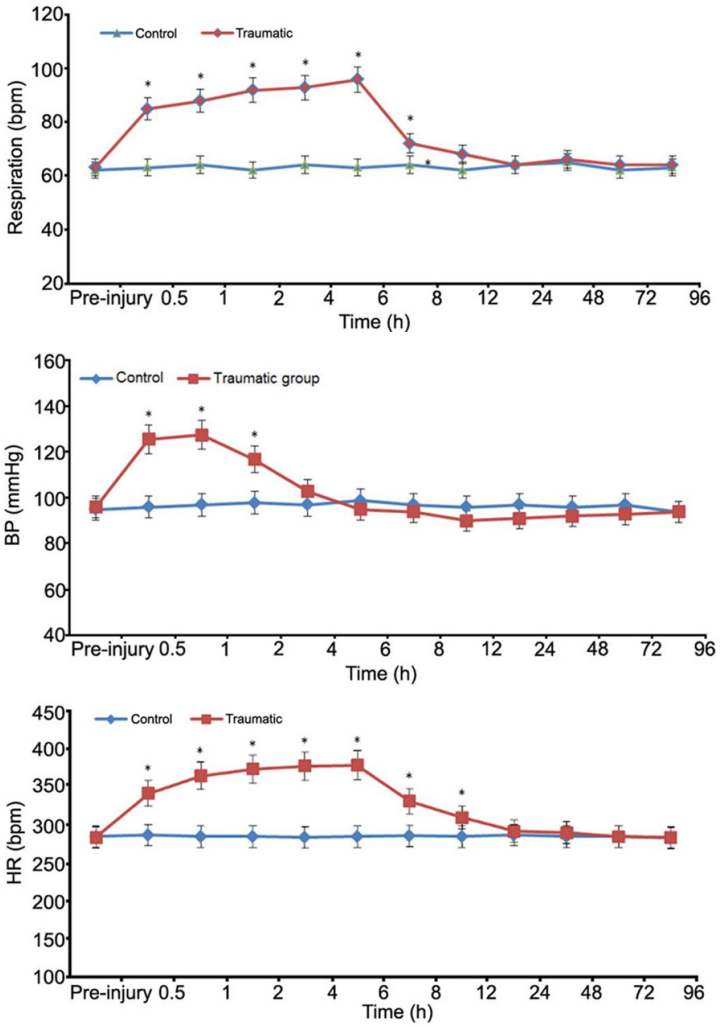

Figure 3. Rat respiration, BP, and HR changes after injury. *P < 0.05, vs control. Rat HR and respiration increased after injury and reached peak at 6 h. They gradually reduced and back to the pre-injury level at 24 h. BP immediately elevated and gradually decreased after 1 h. It was close to pre-injury level after 4 h.

24 h. BP immediately elevated and gradually decreased after 1 h. It was close to pre-injury level after 4 h (**Figure 3**).

PaO_2 changes

PaO_2 level in rats after injury was significantly lower than control ($P < 0.05$). It reached peak at 6 h and then reduced back to pre-injury level after 48 h (**Figure 4**).

Rat LW/DR

LW/DR in rat obviously increased after trauma. It reached peak at 6 h and gradually declined back to pre-injury level at 72 h. LW/DR level at 6, 24, and 48 h after injury was markedly higher than the control ($P < 0.05$) (**Figure 5**).

Lung tissue pathological morphology

HE staining showed that the lung tissue in control exhibited no obvious pathological changes. The cells were in regular arrangement with integrated morphology. No bleeding, edema, or inflammatory cell infiltration was observed in alveolus. The lung tissue in traumatic group exhibited alveolar structure damage, alveolar hemorrhage, alveolar wall thickening, lung tissue edema, and

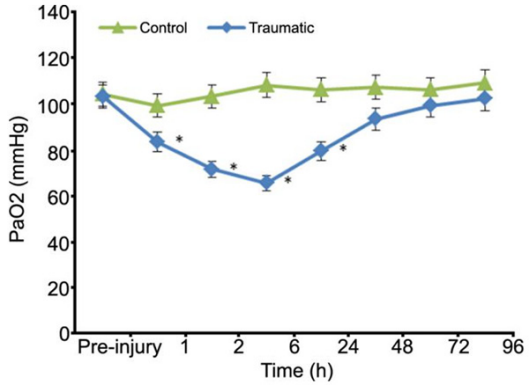

Figure 4. Rat PaO_2 changes. *P < 0.05, vs control.

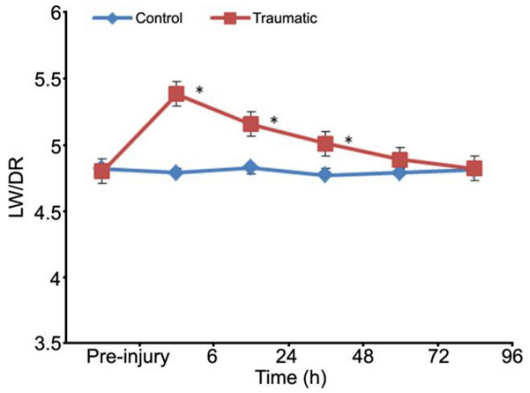

Figure 5. Rat LW/DR. *P < 0.05, vs control.

inflammatory cells infiltration. A large amount of red blood cells were observed in alveolar space and interstitium at 6, 24, and 48 h after injury. They aggravated following time extension (**Figure 6**).

MPO activity and pulmonary microvascular permeability in lung tissue

MPO activity and pulmonary microvascular permeability were significantly higher at 6, 24, 48, and 72 h after injury compared with control (P < 0.05). MPO activity reached peak at 24 h, while microvascular permeability reached peak at 6 h after injury. They gradually decreased after that and got close to pre-injury level at 96 h (**Figure 7**).

VEGF and HIF-1α protein expression in lung tissue

VEGF and HIF-1α protein expressions were obviously higher at 6, 24, 48, and 72 h after injury compared with control (P < 0.05). VEGF and HIF-1α reached peak at 48 h after injury and gradually decreased back to pre-injury level at 96 h (**Figure 8**). VEGF and HIF-1α protein expression presented positive correlation at different time points (r = 0.759, P < 0.05).

Discussion

At present, the related mechanism of traumatic ALI has not been fully elucidated [11, 12]. Most studies applied hemorrhagic shock or endotoxemia /sepsis artery model as animal model, with the disadvantage of cannot fully reflect the characteristics of traumatic ALI [13]. Damage degree should be paid attention in preparation of traumatic ALI model. Too serious primary injury may cause animal died in early period, which cannot observe the secondary injury. Too slight primary injury cannot cause secondary damage. Chest wall deformation and impact velocity in the preparation of traumatic ALI animal model are determined by the driving pressure. Lung tissue damage is associated with driving pressure. This study combined previous simulation results and computer control, thus adopt multi-function biological tapping machine at 350 kpa pressure. It well stimulated the lung trauma, leading the pulmonary contusion mainly in the upper lobe and less involved middle and lower lobes. In addition, since the neighbor organ of right lung tissue is different, different impact site leads to various injury and animal mortality. In order to reduce the impact on the heart damage and circulatory system that may influence the result, this study selected the third and fourth intercostal space in anterior axillary line as the impact point. Impact point shift up may cause axillary artery cleavage and reduce collarbone protection on lung tissue, leading to hemorrhage shock. Impact point shift down will increase the risk of diaphragm and liver rupture, and mainly damage right middle and lower lobes. The incidence of lung injury in traumatic group was 100% and the mortality rate was 48% at 24 h after injury. PaO_2 detection showed hypoxemia. AIS score in rats after injury was 4.16. The lesions were mainly on right upper lobe as bleeding consolidation. Whole lung and local hematoma could be observed. Laceration was found on the surface of lung tissue. Ribs indentation was showed. Right middle and lower lobes were involved in severe case. The lung tissue in traumatic group

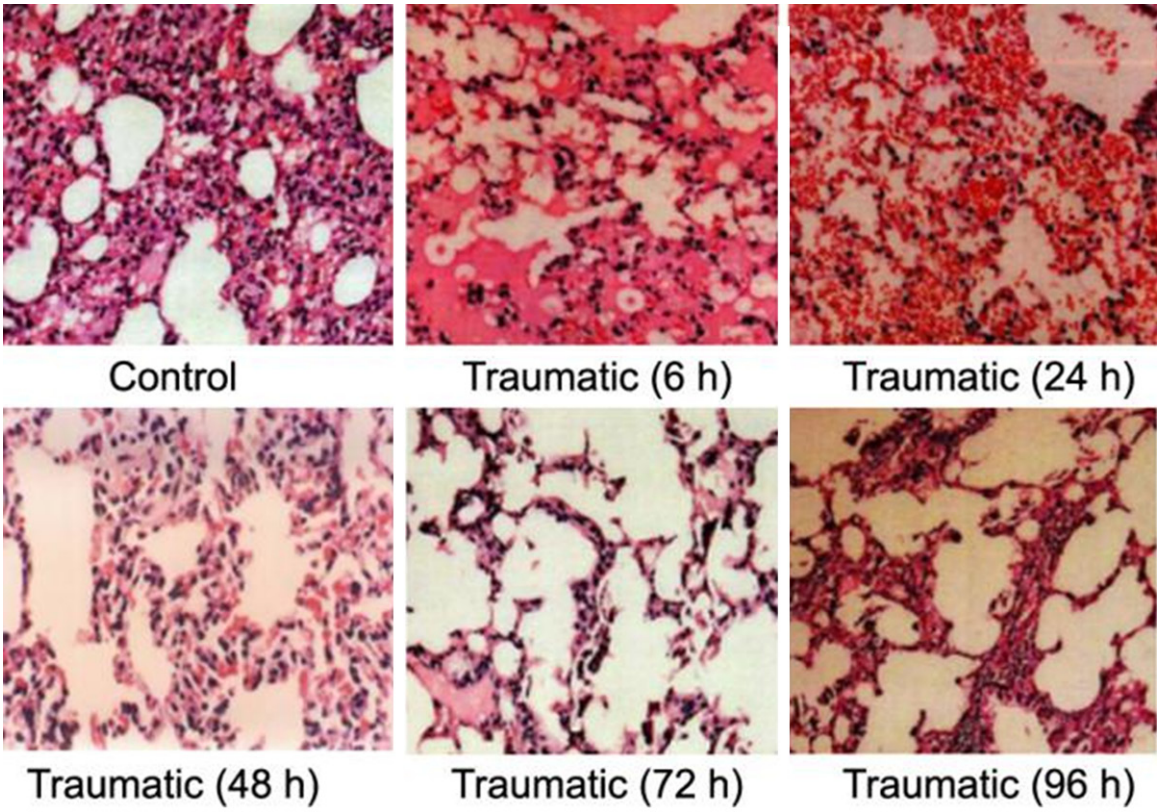

Figure 6. Lung tissue pathological morphology (HE staining ×400).

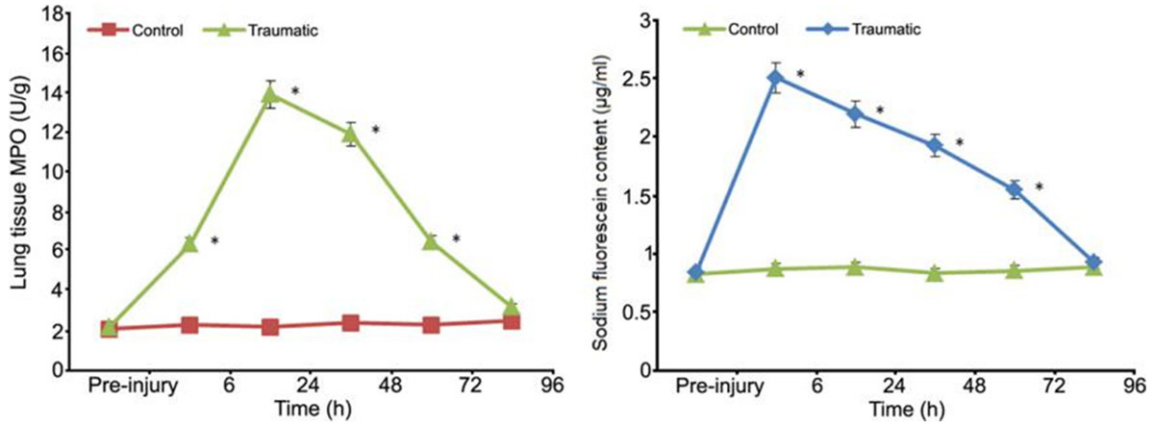

Figure 7. MPO activity and pulmonary microvascular permeability in lung tissue. *P < 0.05, vs control.

exhibited alveolar structure damage, alveolar hemorrhage, alveolar wall thickening, lung tissue edema, and inflammatory cells infiltration. Pulmonary microvascular permeability gradually increased following time extension, suggesting the secondary injury on the basis of primary TLI model, which was in favor of further observation of traumatic ALI mechanism and investigation of corresponding prevention method.

Traumatic ALI is related to multiple factors, such as inflammatory response and apoptosis. ALI induced secondary lesions may be associated with post-traumatic lung tissue hypoxic-ischemia [14, 15]. HIF-1α plays an important role in inflammation, hypoxia, vascular permeability, cell apoptosis, and pulmonary fibrosis after ALI [16, 17]. VEGF shows a critical role in maintaining vascular permeability and angio-

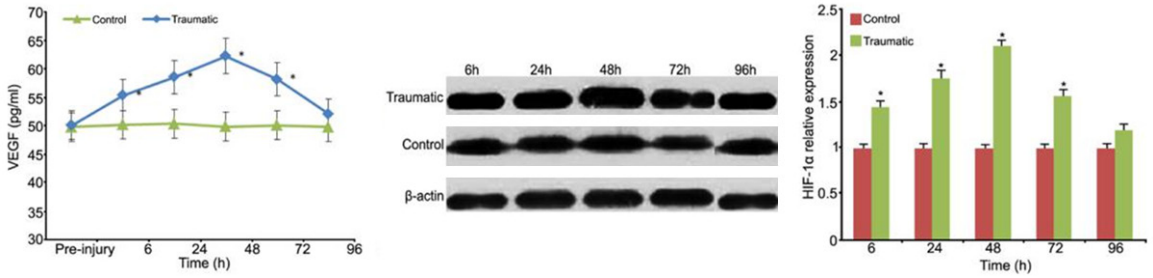

Figure 8. VEGF and HIF-1α protein expression in lung tissue. A: VEGF protein expression. *P < 0.05, vs control. B: HIF-1α protein expression.

genesis. VEGF gene therapy can protect from hyperoxia stimulation in rat. Blocking VEGF signaling pathway can affect lung development in neonatal rat. VEGF overexpresses in lung tissue from endotoxin induced lung injury animal model and is related to pulmonary edema and lung inflammation. VEGF declined in lung tissue from ALI patients, which may be related to alveolar epithelial cell damage degree in ALI. VEGF elevates in alveolar epithelial cells at early inflammation and decreases following inflammatory response aggravation [18, 19]. It was showed that VEGF upregulation in hypoxia was related to HIF-1α. HIF-1α binding site was found in VEGF enhancer. Hypoxia blocks HIF-1α degradation and improves HIF-1α DNA binding activity, leading to HIF-1α overexpression that induces VEGF expression. VEGF acts on vascular endothelial surface receptor to activate ischemia singling pathway [20-22]. VEGF and HIF-1α protein expressions were obviously higher compared with control. VEGF and HIF-1α reached peak at 48 h after injury and gradually decreased back to pre-injury level at 96 h. VEGF and HIF-1α protein expression presented positive correlation at different time points, indicating that HIF-1α may protect cell tolerance to hypoxia and promote injured vascular repair and regeneration through regulating VEGF expression. Pulmonary microvascular regeneration plays a role in the process of tissue damage repair, which may alleviate lung injury to a certain extent. HIF-1α enhances tissue tolerance to hypoxia by regulating VEGF expression. HIF-1α and VEGF participate in the pathophysiological process of lung injury after trauma. This study only explored HIF signaling pathway, whereas HIF-1α may interact with other signaling pathways as an important transcription factor under hypoxia. It still needs further investigation about whether HIF-1α may induce alveolar cell apoptosis in traumatic ALI, which may provide reference to pathogenesis elucidation of ALI/ARDS and lung protection.

Conclusion

HIF-1α and VEGF protein increased after TLI. HIF-1α may protect cell tolerance to hypoxia and promote injured vascular regeneration through regulating VEGF expression.

Acknowledgements

This project supported by the Shandong High School Science & Technology Fund Planning Project (NO. J13LK02).

Disclosure of conflict of interest

None.

Address correspondence to: Dr. Haitao Jiao, Department of Emergency, Eighty-Ninth Hospital of The Chinese People's Liberation Army, 256 North Palace West Street, Weifang 261021, Shandong, China. Tel: +86-536-8439378; Fax: +86-536-8439378; E-mail: haitaojiaozxc@163.com

References

[1] Hitosugi M, Koseki T, Miyama G, Furukawa S, Morita S. Comparison of the injury severity and medical history of disease-related versus trauma-related bicyclist fatalities. Leg Med (Tokyo) 2016; 18: 58-61.

[2] Mokrane FZ, Revel-Mouroz P, Saint Lebes B, Rousseau H. Traumatic injuries of the thoracic aorta: The role of imaging in diagnosis and treatment. Diagn Interv Imaging 2015; 96: 693-706.

[3] Rincon F, Ghosh S, Dey S, Maltenfort M, Vibbert M, Urtecho J, McBride W, Moussouttas M, Bell R, Ratliff JK, Jallo J. Impact of acute lung injury and acute respiratory distress syndrome after traumatic brain injury in the united states. Neurosurgery 2012; 71: 795-803.

[4] Doucet D, Badami C, Palange D, Bonitz RP, Lu Q, Xu DZ, Kannan KB, Colorado I, Feinman R, Deitch EA. Estrogen receptor hormone agonists limit trauma hemorrhage shock-induced gut and lung injury in rats. PLoS One 2010; 5: e9421.

[5] Ji M, Wang Y, Wang L, Chen L, Li J. Protective effect of Xuebijing injection against acute lung injury induced by left ventricular ischemia/reperfusion in rabbits. Exp Ther Med 2016; 12: 51-58.

[6] Xiong LL, Tan Y, Ma HY, Dai P, Qin YX, Yang RA, Xu YY, Deng Z, Zhao W, Xia QJ, Wang TH, Zhang YH. Administration of SB239063, a potent p38 MAPK inhibitor, alleviates acute lung injury induced by intestinal ischemia reperfusion in rats associated with AQP4 downregulation. Int Immunopharmacol 2016; 38: 54-60.

[7] Jin Y, Zhao X, Zhang H, Li Q, Lu G, Zhao X. Modulatory effect of silymarin on pulmonary vascular dysfunction through HIF-1alpha-iNOS following rat lung ischemia-reperfusion injury. Exp Ther Med 2016; 12: 1135-1140.

[8] Lampropoulou V, Sergushichev A, Bambouskova M, Nair S, Vincent EE, Loginicheva E, Cervantes-Barragan L, Ma X, Huang SC, Griss T, Weinheimer CJ, Khader S, Randolph GJ, Pearce EJ, Jones RG, Diwan A, Diamond MS, Artyomov MN. Itaconate links inhibition of succinate dehydrogenase with macrophage metabolic remodeling and regulation of inflammation. Cell Metab 2016; 24: 158-166.

[9] Tong F, Tang X, Li X, Xia W, Liu D. The effect of insulin-loaded linear poly (ethylene glycol)-brush-like poly (l-lysine) block copolymer on renal ischemia/reperfusion-induced lung injury through downregulating hypoxia-inducible factor. Int J Nanomedicine 2016; 11: 1717-1730.

[10] Woik N, Kroll J. Regulation of lung development and regeneration by the vascular system. Cell Mol Life Sci 2015; 72: 2709-2718.

[11] Steinbrenner H, Bilgic E, Pinto A, Engels M, Wollschlager L, Dohrn L, Kellermann K, Boeken U, Akhyari P, Lichtenberg A. Selenium pretreatment for mitigation of ischemia/reperfusion injury in cardiovascular surgery: influence on acute organ damage and inflammatory response. Inflammation 2016; 39: 1363-1376.

[12] Laubach VE, Sharma AK. Mechanisms of lung ischemia-reperfusion injury. Curr Opin Organ Transplant 2016; 21: 246-252.

[13] Tao JQ, Sorokina EM, Vazquez Medina JP, Mishra MK, Yamada Y, Satalin J, Nieman GF, Nellen JR, Beduhn B, Cantu E, Habashi NM, Jungraithmayr W, Christie JD, Chatterjee S. Onset of inflammation with ischemia: implications for donor lung preservation and transplant survival. Am J Transplant 2016; 16: 2598-611.

[14] Jiang X, Khan MA, Tian W, Beilke J, Natarajan R, Kosek J, Yoder MC, Semenza GL, Nicolls MR. Adenovirus-mediated HIF-1alpha gene transfer promotes repair of mouse airway allograft microvasculature and attenuates chronic rejection. J Clin Invest 2011; 121: 2336-2349.

[15] Galvin IM, Steel A, Pinto R, Ferguson ND, Davies MW. Partial liquid ventilation for preventing death and morbidity in adults with acute lung injury and acute respiratory distress syndrome. Cochrane Database Syst Rev 2013; CD003707.

[16] Watanabe Y, Murdoch CE, Sano S, Ido Y, Bachschmid MM, Cohen RA, Matsui R. Glutathione adducts induced by ischemia and deletion of glutaredoxin-1 stabilize HIF-1alpha and improve limb revascularization. Proc Natl Acad Sci U S A 2016; 113: 6011-6016.

[17] Bi LY, Zhao DA, Yang DS, Guo JG, Liang B, Zhang RX, Zhao JL, Bai HT, Li SJ. Effects of autologous SCF-and G-CSF-mobilized bone marrow stem cells on hypoxia-inducible factor-1 in rats with ischemia-reperfusion renal injury. Genet Mol Res 2015; 14: 4102-4112.

[18] Alig SK, Stampnik Y, Pircher J, Rotter R, Gaitzsch E, Ribeiro A, Wornle M, Krotz F, Mannell H. The tyrosine phosphatase SHP-1 regulates hypoxia inducible factor-1alpha (HIF-1alpha) protein levels in endothelial cells under hypoxia. PLoS One 2015; 10: e0121113.

[19] DeNiro M, Al-Mohanna FA. Nuclear factor kappa-B signaling is integral to ocular neovascularization in ischemia-independent microenvironment. PLoS One 2014; 9: e101602.

[20] Di Q, Cheng Z, Kim W, Liu Z, Song H, Li X, Nan Y, Wang C, Cheng X. Impaired cross-activation of beta3 integrin and VEGFR-2 on endothelial progenitor cells with aging decreases angiogenesis in response to hypoxia. Int J Cardiol 2013; 168: 2167-2176.

[21] Ahluwalia A, Tarnawski AS. Critical role of hypoxia sensor--HIF-1alpha in VEGF gene activation. Implications for angiogenesis and tissue injury healing. Curr Med Chem 2012; 19: 90-97.

[22] Zhong Q, Zhou Y, Ye W, Cai T, Zhang X, Deng DY. Hypoxia-inducible factor 1-alpha-AA-modified bone marrow stem cells protect PC12 cells from hypoxia-induced apoptosis, partially through VEGF/PI3K/Akt/FoxO1 pathway. Stem Cells Dev 2012; 21: 2703-2717.